



Research Paper

Munc18b Increases Insulin Granule Fusion, Restoring Deficient Insulin Secretion in Type-2 Diabetes Human and Goto-Kakizaki Rat Islets with Improvement in Glucose Homeostasis



Tairan Qin^{a,1}, Tao Liang^{a,1}, Dan Zhu^{a,1}, Youhou Kang^a, Li Xie^a, Subhankar Dolai^a, Shuzo Sugita^{b,c}, Noriko Takahashi^d, Claes-Goran Ostenson^e, Kate Banks^{b,f}, Herbert Y. Gaisano^{a,b,*}

^a Department of Medicine, University of Toronto, Toronto, ON M5S 1A8, Canada

^b Department of Physiology, University of Toronto, Toronto, ON M5S 1A8, Canada

^c Division of Fundamental Neurobiology, University Health Network, Toronto, ON M5T 2S8, Canada

^d Laboratory of Physiological Chemistry, Institute of Medicinal Chemistry, Hoshi University, Shinagawa, Tokyo 142-8501, Japan

^e Department of Molecular Medicine and Surgery, Endocrinology and Diabetology Unit, Karolinska Institutet, Karolinska University Hospital, SE-171 76 Stockholm, Sweden

^f Division of Comparative Medicine, University of Toronto, Toronto, ON M5S 1A8, Canada

ARTICLE INFO

Article history:

Received 13 June 2016

Received in revised form 9 January 2017

Accepted 20 January 2017

Available online 22 January 2017

ABSTRACT

Reduced pancreatic islet levels of Munc18a/SNARE complex proteins have been postulated to contribute to the deficient glucose-stimulated insulin secretion (GSIS) in type-2 diabetes (T2D). Whereas much previous work has purported Munc18a/SNARE complex (Syntaxin-1A/VAMP-2/SNAP25) to be primarily involved in predocked secretory granule (SG) fusion, less is known about newcomer SGs that undergo minimal docking time at the plasma membrane before fusion. Newcomer SG fusion has been postulated to involve a distinct SM/SNARE complex (Munc18b/Syntaxin-3/VAMP8/SNAP25), whose levels we find also reduced in islets of T2D humans and T2D Goto-Kakizaki (GK) rats. Munc18b overexpression by adenovirus infection (*Ad-Munc18b*), by increasing assembly of Munc18b/SNARE complexes, mediated increased fusion of not only newcomer SGs but also predocked SGs in T2D human and GK rat islets, resulting in rescue of the deficient biphasic GSIS.

Infusion of *Ad-Munc18b* into GK rat pancreas led to sustained improvement in glucose homeostasis. However, Munc18b overexpression in normal islets increased only newcomer SG fusion. Therefore, Munc18b could potentially be deployed in human T2D to rescue the deficient GSIS.

© 2017 The Authors. Published by Elsevier B.V. This is an open access article under the CC BY-NC-ND license (<http://creativecommons.org/licenses/by-nc-nd/4.0/>).

1. Introduction

Insulin secretory granule (SG) fusion with plasma membrane (PM) (*i.e.* exocytosis) releases insulin into the circulation to maintain glucose homeostasis in health (Gaisano, 2014; Rorsman and Renstrom, 2003). In type-2 diabetes (T2D) there are well described defects in insulin exocytosis that prevent β -cells from responding adequately to the increasing glycaemic demand (Hosker et al., 1989). Glucose-stimulated insulin secretion (GSIS) can be affected by increasing the number of insulin SGs reaching and fusing with PM. This process is called primary exocytosis, and this occurs in three modes (Gaisano, 2014). The first mode involves insulin SG docking on PM followed by priming, a biochemical preparation of SGs for release. The SG then sits on PM for long periods awaiting glucose stimulation to cause its exocytotic fusion in the first few

minutes of stimulation. In the second mode of primary exocytosis, insulin SGs from the cell interior are mobilized to PM and undergo fusion after only a short period, or almost no docking time at the PM; these are called newcomer SGs (Ohara-Imaizumi et al., 2007; Shibasaki et al., 2007). Newcomer SGs are responsible for subsequent insulin release after depletion of predocked SGs, and also contribute to a substantial proportion of insulin release in the first few minutes, exceeding the contribution from predocked SGs (Gaisano, 2014; Shibasaki et al., 2007). The third mode of insulin exocytosis, termed compound exocytosis, was first shown many years ago by EM but was largely ignored (Orci and Malaisse, 1980). Endocrine cells such as β -cells seem to require less of this mode and instead exhibit a slower metered and sustained release, primarily effected by increasing primary exocytosis and, when required, release is further increased by restricted sequential fusion of only a few (2 or 3) SGs (Takahashi et al., 2004; Kwan and Gaisano, 2005).

The membrane fusion machinery requires two key components: SNARE (soluble *N*-ethylmaleimide-sensitive factor attachment protein receptor) and Sec1/Munc18(SM) proteins (Kasai et al., 2012). The

* Corresponding author at: University of Toronto, 1 King's College Circle, Rm 7368, Toronto, ON M5S 1A8, Canada.

E-mail address: herbert.gaisano@utoronto.ca (H.Y. Gaisano).

¹ Equal contributors.

SNARE Hypothesis paradigm dictates that different fusion events are mediated by complexes comprising cognate vesicle (v-) SNAREs (vesicle-associated membrane proteins (VAMPs)) and target membrane (t-)SNAREs (syntaxins (Synt) and synaptosome-associated protein of 25 kDa [SNAP25]) (Takahashi et al., 2010, 2015). Assembly of distinct SNARE complexes is regulated by cognate SM proteins to ensure not only their subcellular compartmental specificity, but also that fusogenic actions occur only in response to cellular needs and demand (Jewell et al., 2010; Sudhof and Rothman, 2009). While much is known about the molecular machinery that mediates primary exocytosis of predocked insulin SGs, namely, the neuronal SNARE proteins Syn-1A, SNAP25 and VAMP2, and SNARE complex assembly-modulating proteins, including PKC substrate Syn-1A-binding protein Munc18a (Jewell et al., 2010; Kwan and Gaisano, 2009), much less is known about the molecular machinery that mediates the other exocytotic events, particularly newcomer SG fusion (Gaisano, 2014). The molecular machineries that mediate newcomer SG exocytosis are of importance for increasing insulin secretion in response to increased demand in diabetes and are required to compensate for the defective exocytosis of predocked SGs, which has been shown to at least in part account for reduced first-phase GSIS in T2D (Kwan and Gaisano, 2009; Ohara-Imaizumi et al., 2004). The latter has been attributed to reduced β -cell levels of neuronal SNARE complex and accessory proteins, Munc18a and Munc13-1 (Kwan and Gaisano, 2009; Ostenson et al., 2006).

Munc18 proteins are known to facilitate formation of trans-SNARE complexes that mediate SG fusion (Sudhof and Rothman, 2009). β -cells express all three Munc18 isoforms, Munc18a, b, and c (Oh et al., 2012; Lam et al., 2013; Zhu et al., 2015). We recently reported Munc18c/Syn-4 complex's role in insulin SG exocytosis (Zhu et al., 2015; Xie et al., 2015). We showed Munc18b depletion in rat islets (Lam et al., 2013) disabled the formation of a distinct SNARE complex formation formed by Syn-3 (Zhu et al., 2013) and VAMP8 (Zhu et al., 2012). Munc18b depletion resulted in 50% reduction in primary exocytosis and complete abrogation of the small number sequential SG-SG fusion (Lam et al., 2013). In contrast, gain-of-function expression of Munc18b promoted SNARE complex assembly, which potentiated GSIS in normal rat islets attributed to increased primary exocytosis and to lesser degree enhanced sequential SG-SG fusion, including rarely observed very long-chain (6–8 SGs) fusion (normally only 2–3 SG-SG fusion) (Lam et al., 2013). This raises the possibility that Munc18b-mediated enhancement of exocytosis could be deployed to increase secretory efficiency in T2D.

Animal models of T2D manifest insulin resistance of peripheral tissues (liver, fat, muscle) and insulin secretory defects (Ostenson, 2001). The Stockholm colony of non-obese GK rats, manifest glucose intolerance early in life attributed mainly to β -cell secretory defects, and later (after 3 months) also to progressive reduction of islet mass due to scarring of islets (Ostenson, 2001; Ostenson and Efendic, 2007). GK rats have little insulin resistance that asserts confounding influences on the defective β -cell, and hence represent a cleaner model to examine the β -cell defects *per se* and for testing rescue strategies to restore insulin secretory capacity. The pathogenesis of β -cell secretory defects in GK rats are of polygenic inheritance remarkably well mimicked in human T2D with similar gene expression (Ostenson et al., 2006; Ostenson and Efendic, 2007) and along with susceptibility to further dysfunction by gluco-lipototoxicity which was partially reversible by induced normoglycemic control (Gaisano et al., 2002; Ostenson et al., 2007). Whereas there are many cellular defects (*i.e.* metabolic, cell signaling) in GK rat β -cells contributing to secretory deficiency (Ostenson, 2001), the most prominent is the exocytotic defects *per se*, largely due to the reduced expression of predocked SG SNARE complex (Syn-1A, SNAP-25, VAMP2) and accessory proteins (Munc18a, Munc13-1), which is remarkably well mimicked in islets of T2D patients (Ostenson et al., 2006, 2007; Ostenson and Efendic, 2007; Gaisano et al., 2002). Thus, GK rats are an excellent model of T2D to assess islet secretory deficiency *per se*

and the consequence of rescue by restoration of the deficient exocytotic proteins.

In the current work, we employed a survival surgical technique of infusing virus into the pancreas of GK rats (Banks et al., 2014), ensuring high dosage pancreas-specific expression of components of SM/SNARE complexes (in this study, Munc18b we show to predominantly mediate newcomer SG fusion). We demonstrate that *in vivo* rescue expression of this deficient SM protein into pancreatic islets of T2D GK rats, which would increase SM/SNARE complex formation, could restore insulin secretory capacity sufficient to improve glycemic control; thus representing a potential treatment for T2D.

2. Materials and Methods

2.1. Animals, Pancreatic Islet Isolation and β -cell Culture

Male Goto-Kakizaki rats (original colony obtained from Karolinska Institute, Stockholm, Sweden) were housed in an environmentally controlled room with a 12:12-hour light/dark cycle and allowed *ad libitum* access to standard rat chow and water. Age-matched male Wistar rats served as controls. Animals were cared for and housed in accordance with Canadian Council on Animal Care Standards and the Animals for Research Act of Ontario. All procedures were approved by the University of Toronto Faculties of Medicine and Pharmacy Animal Care Committee.

Pancreatic islets of Langerhans and individuals islet cells were isolated and cultured as previously described (Kwan and Gaisano, 2005) with minor modifications. Islets and β -cells were cultured in RPMI1640 medium with 10% FBS.

2.2. Human Islet

Normal (6 males/8 females; Age: 58.57 ± 4.03 years; BMI: 25.33 ± 0.95 kg/m²; HbA1c: $5.64 \pm 0.08\%$) and T2D human (1 male/6 females; Age: 60.71 ± 4.29 years; BMI: 28.27 ± 2.05 kg/m²; HbA1c: $7.32 \pm 0.73\%$) islets were from IsletCore, University of Alberta, Edmonton, Canada (Table S1). Islets were infected with these viruses: Ad-Munc18b/eGFP, Ad-eGFP, Lenti-Munc18b/mCherry, Lenti-mCherry, Lenti-Munc18b shRNA/CFP or Lenti-CFP; then cultured in 5 mM glucose medium for 48–72 h. Whole islets or dispersed β -cells were assessed. All procedures involving human tissues were approved by Institutional Review Board of the University of Toronto.

2.3. Generation of Adenoviral and Lentiviral Vectors

Munc18b tagged with eGFP in a separate transcription cassette previously reported (Lam et al., 2013; Kauppi et al., 2002) was subcloned into shuttle vector. The resulting plasmid was co-transformed with adenoviral backbone vector pAdEasy-1 into *E. coli* BJ5183 cells to generate recombinant Ad-Munc18b/eGFP virus.

For construction of lentiviruses, Munc18b shRNA-CFP plasmid was created by modifying the parental pLKO-Munc18b shRNA-puro plasmid that we previously described (Han et al., 2009) through replacement of puromycin-resistance gene with CFP. Different core vectors were cotransfected with psPAX2 and pCMV-G into HEK-293FT cells to generate corresponding recombinant lentiviruses: Lenti-Munc18b shRNA/CFP and Lenti-CFP (control); Lenti-Munc18b/mCherry and Lenti-mCherry (control).

2.4. Islet Perfusion and Insulin Secretion Assays

Batches of 50 rat/human islets loaded into perfusion chambers were stimulated with 16.7 mM glucose as previously reported (Zhu et al., 2012), with secreted insulin measured by RIA (EMD Millipore). Insulin secreted was always normalized to total islet insulin content to negate the bias of islet size and β -cell number.

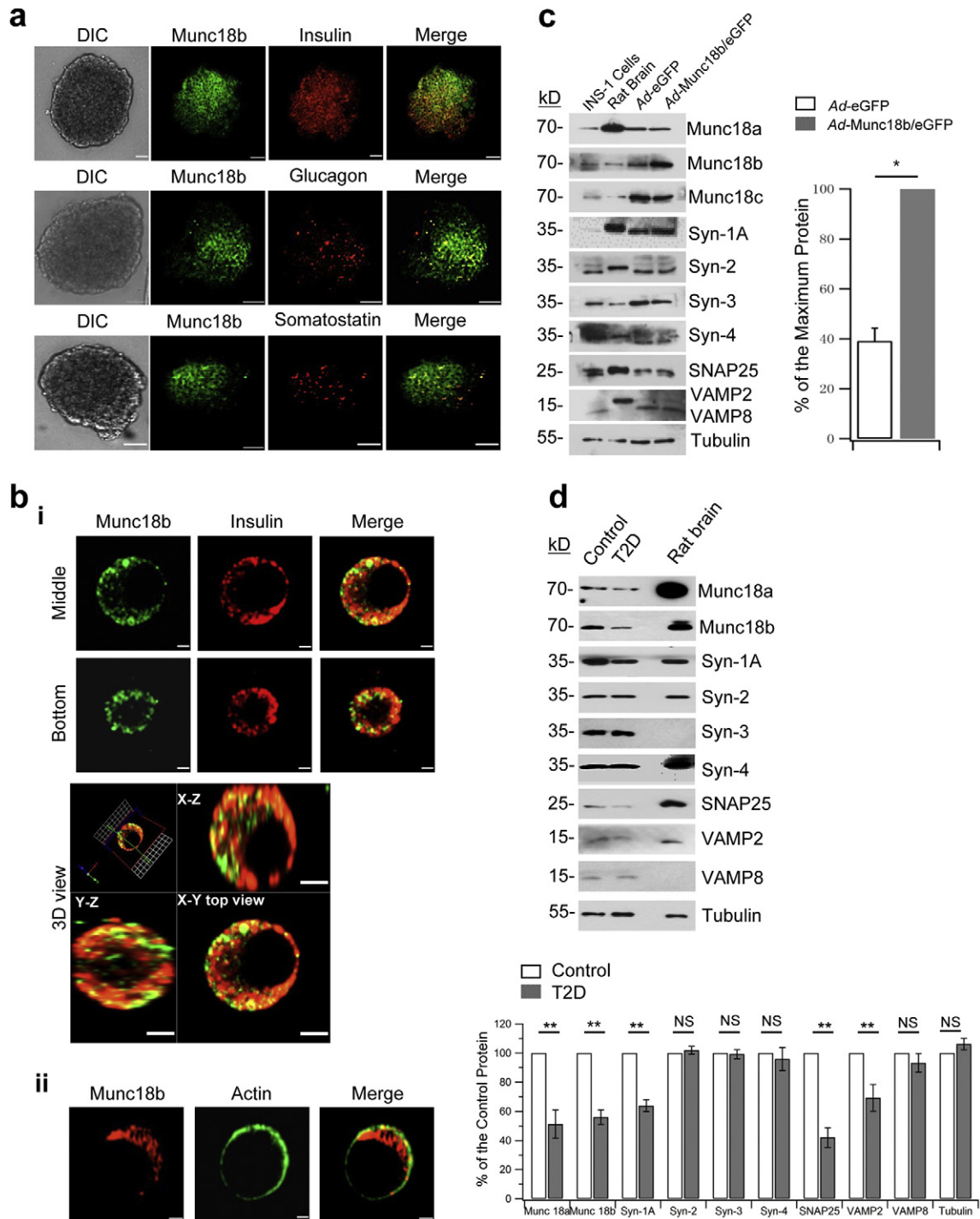


Fig. 1. Munc18b in human β -cells and T2D patient islets. (a) Confocal microscopy showed Munc18b (green) localization to insulin positive β -cells (top), glucagon-positive α -cells (middle) and somatostatin-positive δ -cells (bottom) in human islets. Scale bar: 50 μ m. (b) In dispersed single human islet β -cells, Munc18b (green) is largely located in insulin SGs (i, showing middle and bottom confocal cuts of same cell). Substantial amounts were in the cytoplasm outside the SGs (green in Merge in i, and 3D view, bottom). 3D view is XY, XZ, and YZ cross-sectional views across the middle of the cell shown above. Munc18b also present in PM (ii, with actin). Scale bar: 0.5 μ m. (c) Left: Western blot analysis of SNARE and SM proteins of Ad-Munc18b/eGFP and Ad-eGFP transduced normal human islets. Right: Densitometric analysis showing 2.56 fold Munc18b overexpression compared to normal levels (N = 3). Expression of other proteins was not affected by Munc18b overexpression (analysis data not shown). Data shown is representative of 3 separate experiments. (d) Western blots of islets from T2D patient donors compared to normal human islets. Graphical analysis (bottom) of Munc18b and SNARE proteins (N = 3). Data are shown as mean \pm SEM, *p < 0.05; **p < 0.01; NS: no significant difference.

2.5. Confocal Immunofluorescence Microscopy

This was performed as previously described (Zhu et al., 2012). Islets were washed with PBS, fixed in 4% paraformaldehyde in PBS for 45 min, and permeabilized in 0.2% Triton X-100 buffer for 60 min at 37 $^{\circ}$ C. Islets

were labeled with primary antibodies and corresponding secondary antibodies, or directly checked for transduced fluorescent protein signals. Islets mounted on glass coverslips were examined using a Olympus IX81 inverted microscope coupled to a Yokogawa CSU X1 spinning disk confocal scan head (Olympus Co., Tokyo, Japan) and Hamamatsu

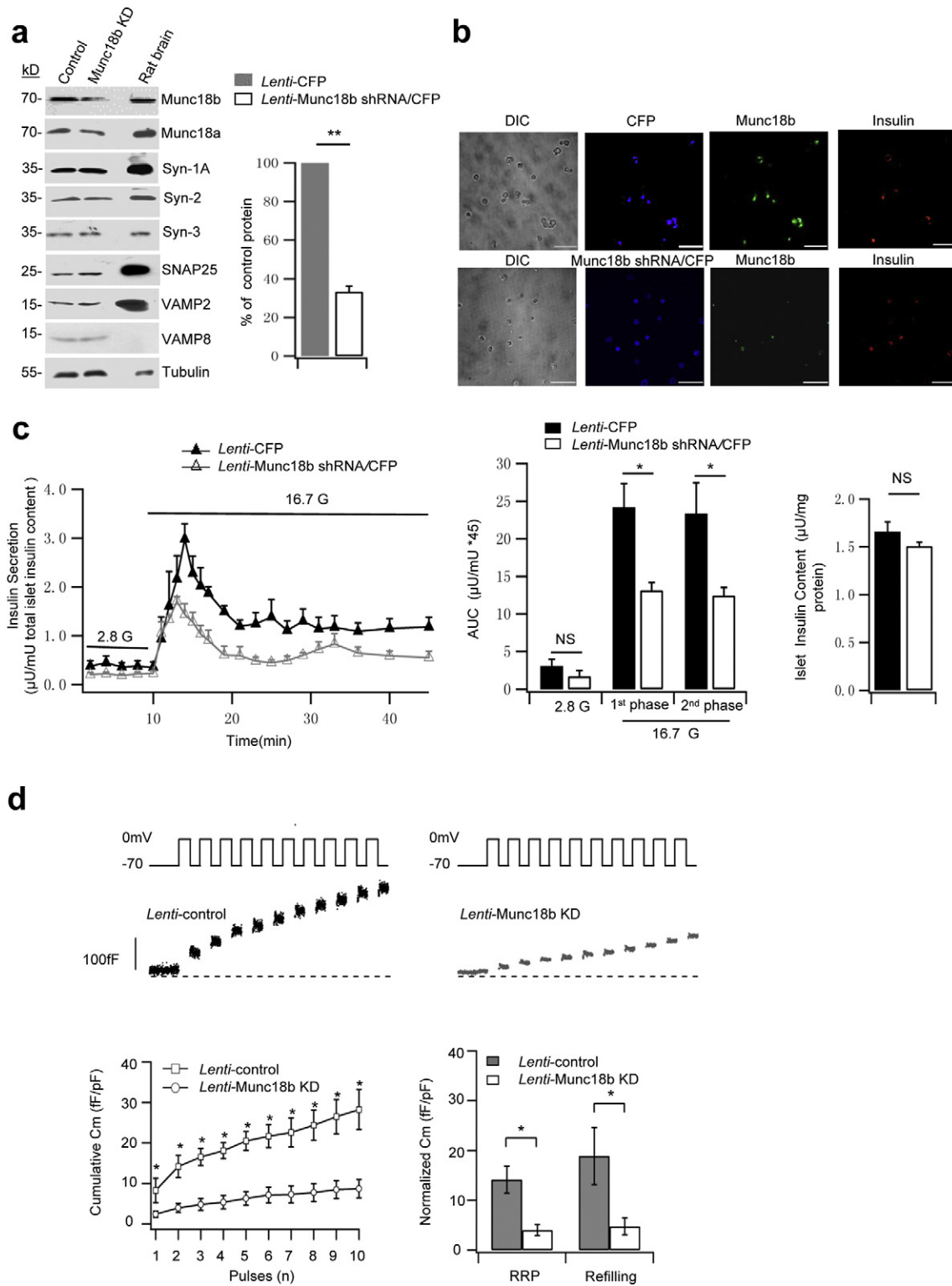


Fig. 2. Munc18b depletion decreases biphasic GSIS in human islets. (a) Western blot analysis of *Lenti-Munc18b* shRNA/CFP-induced knockdown of Munc18b expression on normal human islets; representative of 3 experiments. *Right*: Densitometric analysis of the reduction of Munc18b normalized to percentage of control (N = 3); there was no change in any of the other proteins after Munc18b KD, therefore analysis not shown. (b) Islets transduced with *Lenti-Munc18b* shRNA/CFP (*bottom*) or *Lenti-CFP* (*top*) were dispersed to single cells, then triple labeled with CFP (assigned blue color), Munc18b/Cy5 (assigned green color) and insulin/TxRed (red color). Scale bar: 100 μ m. (c) Islet perfusion assays on *Lenti-Munc18b* shRNA/CFP- vs *Lenti-CFP*-transduced normal human islets; corresponding AUCs analysis of first- (10–25 min) and second-phase (25–45 min) GSIS (*middle*) and total islet insulin content (*right*). N = 4 human islet donors. (d) Cm recording performed on single human β -cells (CFP-positive) infected with *Lenti-Munc18b* shRNA/CFP (N = 8) or *Lenti-CFP* (N = 6). *Top*: Representative recordings of Δ Cm. *Bottom left*: Cumulative changes in Cm normalized to basal cell Cm (ff/pF). *Bottom right*: Summary of RRP (Δ Cm_{1st–2nd} pulses) and rate of SG refilling (Δ Cm_{3rd–10th} pulses). Data are shown as mean \pm SEM, *p < 0.05; **p < 0.01, NS: no significant difference.

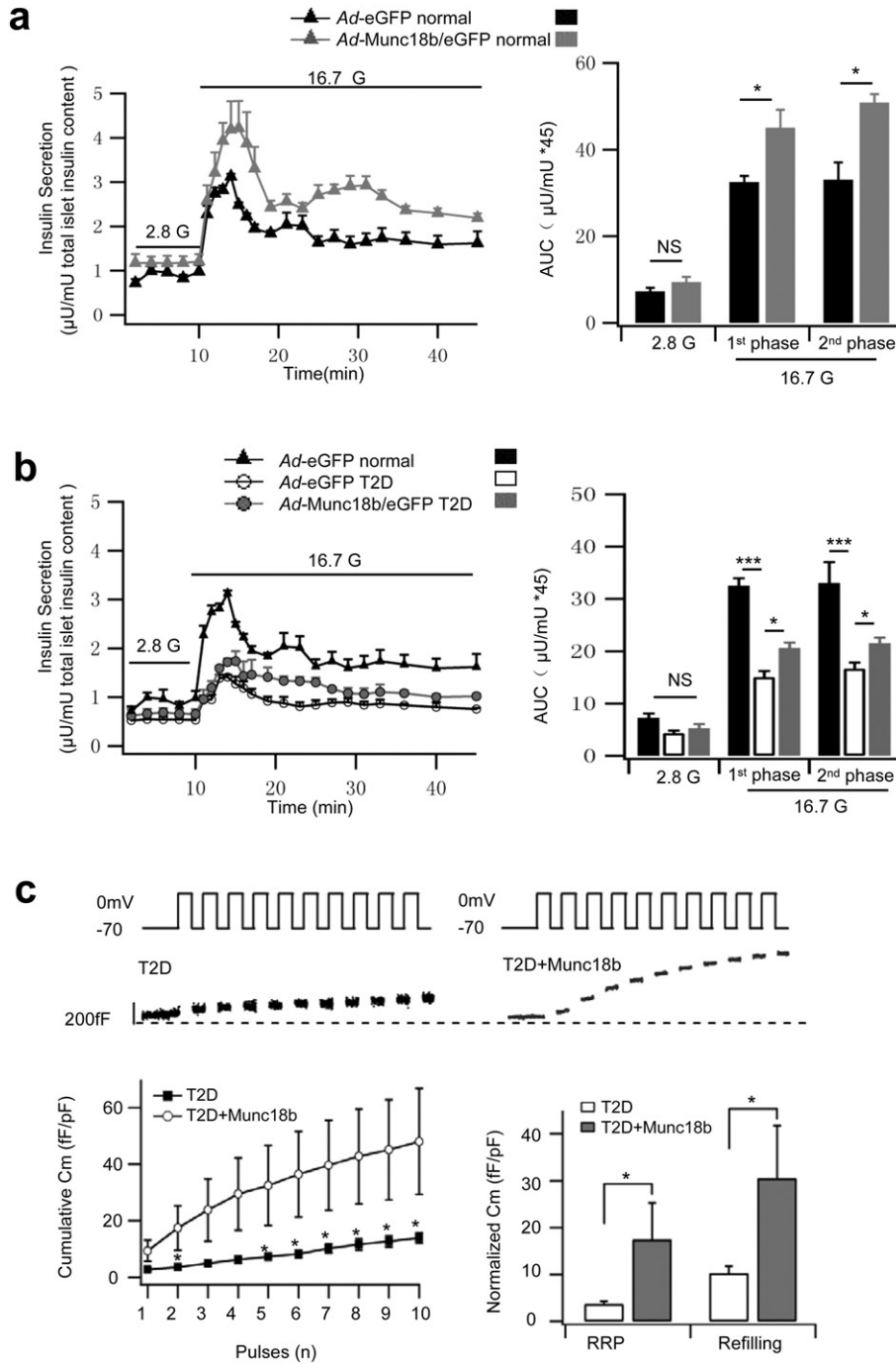


Fig. 3. Munc18b overexpression rescues the deficient insulin secretion from pancreatic islets of type 2 diabetic patients. (a–b) Islet perfusion assays of (a) *Ad-Munc18b/eGFP*- vs *Ad-eGFP*-transduced normal human islets (N = 4 human islet donors); (b) *Ad-eGFP*-transduced normal (N = 4 from A) vs T2D human islets (N = 3 donors) vs *Ad-Munc18b/eGFP*-transduced T2D human islets (N = 3 donors). On the right are AUCs (area under the curve) summaries of the first- (10–25 min) and second-phase GSIS (25–45 min). (c) Cell membrane capacitance (Cm) recordings from T2D human pancreatic β-cells transduced with *Lenti-Munc18b/mCherry* (N = 7) vs *Lenti-mCherry* (Control, N = 10). Top: Representative recordings of ΔCm during a train of ten 500-ms depolarizations from –70 mV to 0 mV. Bottom left: Cumulative changes in Cm normalized to basal cell Cm (fF/pF). Bottom right: Summary of RRP (ΔCm_{1st–2nd} pulses) and rate of SG refilling (ΔCm_{3rd–10th} pulses). Data are shown as mean ± SEM, *p < 0.05; ***p < 0.001, NS: no significant difference.

EM-CCD (Bridgewater, NJ). Data acquisition and analysis were performed using Volocity software (PerkinElmer, Waltham, MA).

2.6. Western Blotting

72 h after infection, human and rat islets were collected, whole cell lysate proteins separated on 12/15% SDS-PAGE, proteins then transferred to nitrocellulose membrane and identified with the following

antibodies: Munc18a (1:1000; BD Transduction Laboratories, San Jose, CA), Munc18b (1:800; V. Oikkonen, Minerva Foundation Institute, Helsinki, Finland) (Riento et al., 1996; Lam et al., 2013); Munc18c (1:800; D. Thurmond, City of Hope, Duarte, CA); Syn-1A (1:1500; Sigma Co., St. Louis, MO); SNAP-25 (1:1500; Sternberger Monoclonal, Covance, Princeton, NJ), VAMP2 (1:500; A. Lowe, Stanford University, Stanford, CA), VAMP8 (1:500; CC. Wang and WJ Hong, Institute of Molecular and Cell Biology, Singapore); and from Synaptic Systems

(Goettingen, Germany) include Syn-2 (1:1200), Syn-3 (1:800), Syn-4 (1:1500), SNAP-23 (1:1000) and anti-tubulin (1:1000). Noncommercial antibodies for VAMP2, VAMP8 and Munc18b were validated in our previous papers (Zhu et al., 2012). Blots were quantified by densitometry scanning followed by analysis with Scion Image (release BETA 4.0.2, Scion Corp.).

2.7. Pancreatic Ductal Injection

A surgical technique (Banks et al., 2014) was employed to infuse Ad-Munc18b/eGFP (400 μ L saline (with methylene blue) containing 9.4×10^{12} pfu of virus infused at a rate of 50 μ L/min) into the entire pancreas, thus ensuring high dosage pancreas-specific expression of the viral construct. This was achieved by retrograde infusion into the common biliopancreatic duct during temporary occlusion of the common bile duct. For acute study, pancreas was resected 2 h post-infusion without recovery, islets then isolated and cultured for 2 days to monitor expression of the translated Munc18b proteins. For the chronic survival study, rats were recovered with an appropriate analgesic plan, with abdominal closure in 2 layers; absorbable sutures into the muscle layer and stapling of the skin. The rats were nursed back to full recovery prior to subsequent IPGTT and ITT studies, done at the earliest at 1 week postoperatively.

2.8. Intraperitoneal Glucose Tolerance Test (IPGTT) and Insulin Tolerance Test (ITT)

IPGTTs (2 g glucose/kg b.w.) were performed at 1, 2, 4, 8 and 16 weeks post-operatively following an 18 h fast, with both blood glucose and insulin levels determined by RIA kit (EMD Millipore). ITT was conducted with intraperitoneal injection of human biosynthetic insulin (0.5 units/kg b.w., Eli Lilly Canada) after a 6 h fast; a drop of blood obtained from tail vein at indicated times was obtained for glucose determination.

2.9. Electrophysiology

Patch electrodes were pulled from 1.5 mm thin-walled borosilicate glass, coated close to the tip with orthodontic wax, and polished to a tip resistance of 2–3 M Ω when filled with intracellular solution. For measurement of C_m , intracellular solution contains (in mM): 125 Cesium glutamate, 10 CsCl, 10 NaCl, 1 MgCl₂, 5 HEPES, 0.05 EGTA, 3 MgATP, and 0.1 cAMP (pH 7.2). The extracellular solution contains (in mM): 118 NaCl, 5.6 KCl, 1.2 MgCl₂, 10 CaCl₂, 20 tetraethylammonium chloride, 5 HEPES, and 5 D-glucose (pH 7.4). C_m was estimated by the Lindau-Neher technique, implementing the “Sine-DC” feature of the Lock-in module (40 mV peak-to-peak and a frequency of 1 kHz) in whole-cell configuration. Large round cells were chosen as β -cells. Recordings were conducted using an EPC10 patch clamp amplifier and using Pulse and X-chart software programs (HEKA Elektronik). Exocytic events were elicited by a train of ten 500-ms depolarization pulses from –70 mV to 0 mV. All recordings were performed at 30 °C.

2.10. Total Internal Reflection Fluorescence (TIRF) Microscopy Imaging of Insulin Exocytosis

This was performed with a Nikon TIRF microscope system (Tokyo, Japan) as previously reported (Zhu et al., 2012, 2013). A monolayer of β -cells under indicated conditions were infected with adenovirus neuropeptide Y (NPY)-eGFP and cultured for 24 h before performing TIRF recording. Large round cells were chosen as β -cells which were confirmed by their response to high glucose stimulation. Fusion events, indicated by abrupt brightening of NPY-eGFP fluorescence, were manually selected, analyzed and categorized into ‘predocked’ (docked on PM at basal, then fuses after stimulation) and ‘newcomer’ SGs (not predocked on PM at basal), the latter divided into ‘short dock’ (short

residence time of >200 ms at the PM) or ‘no dock’ (<200 ms at the PM, which is the interval of one frame) (Zhu et al., 2012, 2013).

2.11. Islet Histological Analysis of GK Rat Pancreas

Pancreatic tissue from GK rats was cut to 7 μ m-thick sections at the head, middle and tail of pancreas and stained for insulin (Dako) as dicribled previously (Zhu et al., 2012). Insulin-immunostained sections were scanned using a Zeiss Axioscan Slide Scanner and analyzed with Zeiss Zen lite software (Carl Zeiss).

2.12. Statistical Analysis

All data are presented as mean \pm SEM. Statistical significance was assessed by repeated measure ANOVA, independent-samples *t*-test or Mann-Whitney *U* test using SPSS (IBM). Significant difference is indicated by asterisks (**p* < 0.05, ***p* < 0.01, ****p* < 0.001).

3. Results

3.1. Munc18b is Abundant in Human β -cells

In human islets, Munc18b is present not only in β -cells (Fig. 1a, top images), but also in glucagon-positive α -cells (Fig. 1a, middle images) and somatostatin-positive δ -cells (Fig. 1a, bottom images). Within dispersed human β -cell, Munc18b is abundant not only on insulin SGs (Lam et al., 2013) observed in different sections of the β -cell (Fig. 1bi), consistent with our previous report in rat β -cells (Lam et al., 2013). However, we also noted very substantial amounts of Munc18b in the cytoplasm outside the SGs (green in ‘merge’ images, Fig. 1bi and 3D view) and only small amounts on the PM (colocalized with actin in Fig. 1bii). Western blots of human islets (Fig. 1c, d) confirmed the abundance of Munc18b and its cognate SNARE complex proteins (Syn-3, VAMP8, VAMP2) (Lam et al., 2013; Zhu et al., 2012, 2013), as well other SM/SNARE complexes (Oh et al., 2012; Zhu et al., 2015; Xie et al., 2015) known to mediate insulin secretion.

3.2. Munc18b Depletion Decreases Biphasic GSIS in Human Islets

We first assessed the endogenous function of Munc18b in human β -cells by depleting Munc18b levels in normal human islets employing *Lenti*-shRNA knockdown. Western blots of infected islets (Fig. 2a, *Lenti*-Munc18b shRNA/CFP vs *Lenti*-CFP control) showed a reduction of Munc18b levels by 67%, whereas levels of syntaxins, VAMPs, SNAP25 and Munc18a proteins were not altered by Munc18b deletion. This would indicate the secretory effects observed in subsequent studies are attributed solely to Munc18b depletion *per se* or its actions on SNARE complex assembly. Fig. 2b confirmed the high transfection efficiency wherein 89% of cells infected with the viruses were CFP-positive (of 1311 cells detected by phase contrast, 1166 cells expressed CFP). Insulin staining revealed that 93% of β -cells were infected with the viruses (of 875 insulin-positive β -cells, 813 cells expressed CFP). While most Munc18b shRNA/CFP-tagged cells were completely depleted of Munc18b, a few Munc18b shRNA/CFP-tagged cells still contained small residual Munc18b (Fig. 2b bottom showed reduced Munc18b/GFP fluorescence intensity compared with CFP-infected control cells in Fig. 2b top). Fig. 2c shows that Munc18b depletion reduced first-phase GSIS by 46% (Munc18b shRNA: 13.13 ± 1.46 ; CFP control: 24.19 ± 3.15) and second-phase GSIS by 47% (Munc18b shRNA: 12.43 ± 1.91 ; CFP control: 23.36 ± 4.07). This reduction in GSIS is not due to any effects on insulin biosynthesis (Fig. 2c right). In contrast to the islet secretion study, single cell analysis of CFP-tagged β -cells would assess only Munc18b-depleted cells. We therefore performed patch clamp capacitance measurements (C_m) of CFP-fluorescent cells (Fig. 2d) to estimate the size of the readily releasable pool (RRP, first two depolarization pulses, $\Delta C_{m1st-2nd}$) and rate of refilling of RRP from the reserve pool

(3rd to 10th depolarization pulses, $\Delta C_{m_{3rd-10th}}$). This notion was previously purported (now considered inappropriate) to correspond to first- and second-phase GSIS, respectively (Rorsman and Renstrom, 2003). C_m increases in Munc18b-depleted β -cells was greatly inhibited at every depolarizing pulse, wherein the size of the RRP was reduced by 72% (Munc18b shRNA: 4 ± 1.1 fF/pF; CFP control: 14.2 ± 2.7 fF/pF) and rate of SG refilling/mobilization reduced by 75% (Munc18b shRNA: 4.7 ± 1.7 fF/pF; CFP control: 18.9 ± 5.7 fF/pF).

3.3. Munc18b Overexpression Not Only Increases Biphasic GSIS in Normal Human Islets and but Can Rescue the Deficient GSIS in Islets of T2D Patients

We performed to converse study of overexpressing Munc18b in human islets employing *Ad-Munc18b/eGFP*, which increased human islet Munc18b levels to a moderate 2.6 fold of normal islet levels. Munc18b overexpression did not affect the levels of other Munc18 or SNARE proteins (Fig. 1c), but resulted in an increase in biphasic GSIS (16.7 mM glucose, Fig. 3a) with first-phase GSIS increased by 39% (*Ad-Munc18b/eGFP*: 45.06 ± 4.13 ; *Ad-eGFP*: 32.50 ± 1.43) and second-phase increased by 54% (*Ad-Munc18b/eGFP*: 50.89 ± 1.97 ; *Ad-eGFP*: 33.03 ± 4.02).

Human T2D diabetes islets exhibit reduced levels of cognate Munc18a, Syn-1A, VAMP2 and SNAP25 (Ostenson et al., 2006) which we here reassessed (Fig. 1d). Munc18b levels were similarly reduced as Munc18a (51% of normal) to 56% of normal levels. Cognate Syn-3 and VAMP8 levels in T2D human islets were however normal (Fig. 1d). This suggests that additional Munc18b could potentially activate sufficient amounts of these normal levels of cognate SNARE proteins to assemble into complexes to promote insulin secretion. Fig. 3b shows the effects of *Ad-Munc18b/eGFP* rescue of deficient human T2D islet Munc18b levels in restoring the deficient GSIS. We first compared the GSIS of normal and T2D human islets (Fig. 3b), whereby human T2D islets exhibited a 54% reduction in first-phase GSIS (normal: 32.50 ± 1.43 ; T2D: 15.04 ± 1.18) and 50% reduction in second-phase GSIS (normal: 33.03 ± 4.02 ; T2D: 16.66 ± 1.12). *Ad-Munc18b/eGFP* infection of T2D human islets effected a moderate rescue of this deficient GSIS by increasing first-phase GSIS by 37% (*Ad-Munc18b/eGFP*: 20.61 ± 1.03 ; *Ad-eGFP* control: 15.04 ± 1.18) and second-phase GSIS by 29% (*Ad-Munc18b/eGFP*: 21.53 ± 1.09 ; *Ad-eGFP*: 16.66 ± 1.12). We were constrained by the small number of available T2D human islets per shipment; therefore did not have enough T2D human islets to perform Westerns to determine how much Munc18b levels were increased by the adenovirus. This can be estimated from ~2.6 fold of Munc18b levels in normal islets infected with *Ad-Munc18b/eGFP* (Fig. 1c) plus the 56% Munc18b levels in T2D human islets (Fig. 1d), which would add up to ~150% of Munc18b levels in the *Ad-Munc18b/eGFP*-infected human T2D islets.

We next examined the insulin SG populations affected by *Lenti-Munc18b/mCherry* overexpression that would account for this increase in first- and second-phase GSIS. mCherry fluorescence identifies Munc18b-overexpressing cells (*Lenti-mCherry* used as control). Munc18b overexpression in human T2D β -cells increased capacitance at every depolarizing pulse compared with the rather depressed exocytotic responses in control T2D β -cells (Fig. 3c). Munc18b overexpression increased RRP size by 379% (Munc18b/mCherry: 17.5 ± 7.8 fF/pF;

mCherry: 3.65 ± 0.66 fF/pF) and rate of refilling increased by 196% (Munc18b/mCherry: 30.5 ± 11.2 fF/pF; mCherry: 10.3 ± 1.5 fF/pF). The apparent discrepancy between the large C_m increases and the more moderate increases in first- and second-phase GSIS by islet perfusion assay is largely attributed to the many large T2D islets which reduced the ability of the virus to reach the islet cores compared to the higher infection efficiency of normal human islets. In contrast, the Munc18b levels in each Munc18b/mCherry-tagged β -cell assessed by C_m assay were higher than the whole islet protein levels. Whereas electrical depolarization protocols are suprphysiologic compared to glucose stimulation, and are independently useful in deciphering different secretory kinetics, these assays should not be extrapolated to each other as they have very different time courses. Nonetheless, the large C_m increases from the infected β -cells would suggest a near-complete rescue of the deficient biphasic GSIS from the human T2D islets.

3.4. Munc18b Restores Exocytosis of Predocked and Newcomer SGs in T2D Human β -cells

We next examined which population of insulin SGs were specifically influenced by Munc18b by time-lapse total internal reflection fluorescence microscopy (TIRFM) of insulin SGs tagged with neuropeptide Y (NPY)-eGFP (*Ad-NPY-eGFP*). On TIRFM, SG populations could be segregated into those docked at PM for some time before stimulated to undergo fusion (predocked SGs) and newcomer SGs that undergo minimal (few seconds to few minutes, short dock SGs) to no docking time (no dock SGs) at PM before fusion (Gaisano, 2014). The population of no dock newcomer SGs is much larger than the short dock SGs (Gaisano, 2014), which we have combined in our calculations below. While considerable insights have been reported on mediators involved in newcomer SG fusion using TIRFM (Gaisano, 2014), elucidation of the full molecular mechanism of newcomer SGs by TIRFM is insufficient since TIRFM cannot see the behaviour of these SGs before they dock onto the PM.

At rest, the density of predocked SGs on the PM was reduced in the T2D human β -cells (T2D: 8.35 ± 0.40 ; normal: 12.20 ± 0.82 , Fig. 4a), which in part explains a 70% reduction in fusion of predocked SGs compared to normal human β -cells (T2D: 1.70 ± 0.52 ; normal: 5.61 ± 0.80 , Fig. 4bi, ii, analysis in iv). Munc18b overexpression by *Lenti-Munc18b/mCherry* expression increased the density of predocked SGs (T2D + Munc18b: 10.00 ± 0.63 ; T2D: 8.35 ± 0.40 , Fig. 4a), which would increase the availability of predocked SGs to undergo fusion. Indeed, in the first 5 min of stimulation (designated as first-phase), Munc18b overexpression rescued the number of predocked SG fusion (T2D + Munc18b: 4.43 ± 0.93 ; T2D: 1.70 ± 0.52) to similar levels as normal human β -cells (see summary graph in Fig. 4biv). The effect of Munc18b on predocked SGs was somewhat surprising as we had presupposed that predocked SG fusion to be mediated by Munc18a acting on Syn-1A and VAMP2 (Sudhof and Rothman, 2009; Oh et al., 2012), which are depleted in T2D β -cells (Fig. 1d).

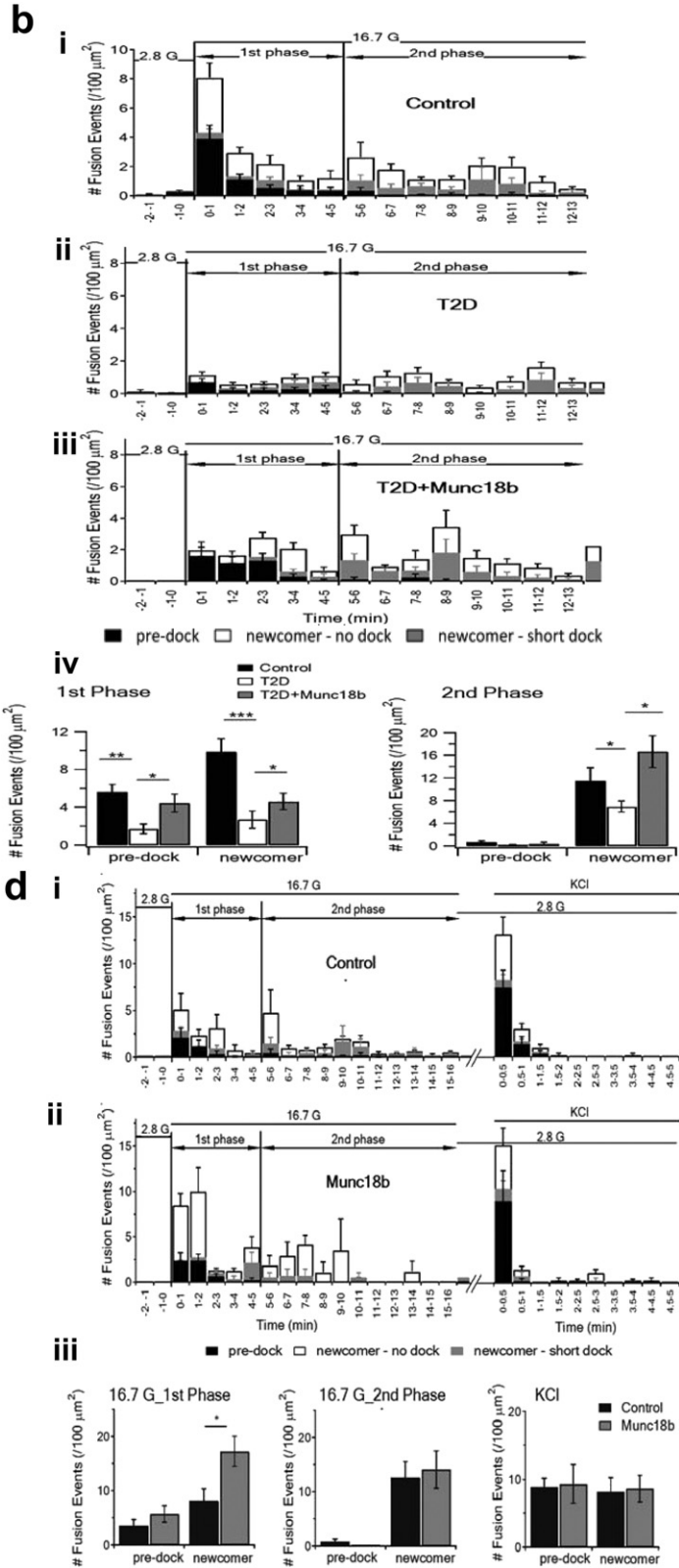
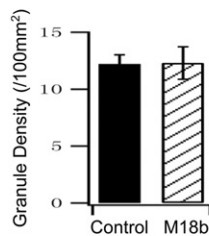
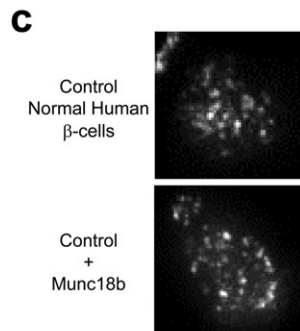
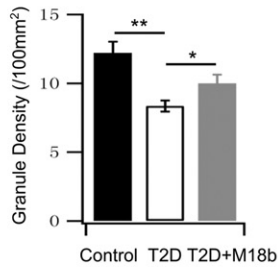
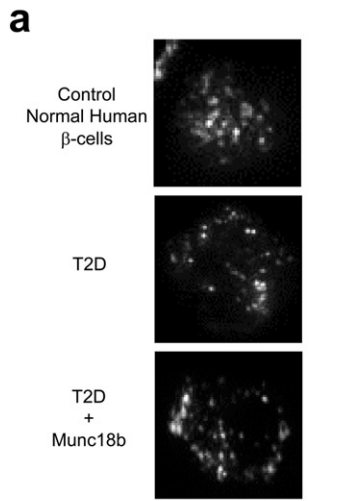
During the first 5 min of stimulation (first-phase), we saw a 73% reduction in newcomer SGs (T2D: 2.69 ± 0.89 ; normal: 9.86 ± 1.38), and after 5 min stimulation (5–13 min, designated as second-phase), T2D β -cells showed a 40% reduction in newcomer SGs (T2D: 6.93 ± 0.97 ; normal: 11.48 ± 2.33). Remarkably, *Lenti-Munc18b/mCherry* expression into T2D human β -cells (Fig. 4biii, iv) rescued newcomer SGs in first-

Fig. 4. Munc18b rescues biphasic GSIS in T2D human islets by restoring exocytosis of predocked and newcomer SGs. TIRFM images (graphical analysis, bottom) SG density on the PM at basal condition (a–b) TIRFM images of SG density on the PM at basal condition (a) and histograms of SG fusion events during glucose-stimulated conditions (b) of T2D human β -cells. (a) SG density at resting condition (N = 12). Scale bars represent 2 μ m. Bottom: Comparison of averaged SG densities. (b) Different glucose-stimulated fusion events in first-phase (first 5 min after 16.7 mM glucose stimulation) and second-phase (5–13 min) in control normal human β -cells (i, N = 15), T2D human β -cells transduced with *Lenti-mCherry* (ii, N = 18) or T2D human β -cells transduced with *Lenti-Munc18b/mCherry* (iii, N = 19). Data obtained from 3 independent experiments. (iv) Although (ii) and (iii) are shown in the three modes of fusion (predocked, short-dock and no-dock newcomer SGs) events in first- and second-phase GSIS, the summary combined the two populations of newcomer SGs. (c–d) TIRFM images showing the SG density on the PM at basal condition (c; N = 8; scale bars represent 2 μ m; Bottom: Comparison of averaged SG densities) and histograms of SG fusion events at glucose-stimulated conditions of normal human β -cells (d). Normal human β -cells were transduced with *Lenti-mCherry* (i, control, N = 16) or *Lenti-Munc18b/mCherry* (ii, N = 17) and stimulated with 16.7 mM glucose followed by 40 mM KCl (right). Data obtained from 3 independent experiments. (iii) Although (i) and (ii) are shown in the three modes of fusion (predocked, short-dock and no-dock newcomer SGs) events in first- and second-phase GSIS, the summary combined the two populations of newcomer SGs, including the KCl stimulation. Data are shown as mean \pm SEM, *p < 0.05; **p < 0.01, ***p < 0.001.

phase by 82% (T2D + Munc18b: 4.90 ± 0.87 ; T2D: 2.69 ± 0.89) approaching 50% of normal (9.86); and in second-phase by 140% (T2D + Munc18b: 16.64 ± 2.81 ; T2D: 6.93 ± 0.97), which exceeded normal secretion (by 45%, normal being 11.48).

We then overexpressed Munc18b-mCherry in normal human β -cells (Fig. 4c, d). At rest, there was no difference in the density of

predocked SGs after Munc18b overexpression (normal: 12.20 ± 0.82 ; normal + Munc18b: 12.30 ± 1.43 , Fig. 4c). During glucose stimulation, we saw similar increases as in the T2D human β -cells in first-phase (normal + Munc18b: 17.26 ± 2.79 ; normal: 8.16 ± 2.16), but no increase in second-phase as was seen in T2D human β -cells. More importantly and in contrast to human T2D β -cells, there was no



increase in predocked SG fusion (Fig. 4d, normal + Munc18b: 5.70 ± 1.54 ; normal: 3.61 ± 1.07). To be certain that predocked SGs in normal β -cells were insensitive to Munc18b overexpression, 40 mM KCl depolarization, known to more preferentially evoke release of predocked SGs, was not different between Munc18b/mCherry-expressing and control β -cells.

We interpret these findings as follows. First, Munc18b is the putative SM protein that mediates exocytosis of newcomer SGs, by preferentially activating Syn-3/VAMP8/SNAP25 SNARE complexes (Lam et al., 2013). Second, Munc18b also binds Syn-1A (Lam et al., 2013), albeit Syn-1A levels were limiting in T2D β -cells, thus could replace Munc18a's actions in increasing the number of predocked SGs on the PM when Munc18a is deficient in T2D β -cells. Munc18b overexpression could therefore compensate for Munc18a deficiency in T2D β -cells, supporting the thinking of functional redundancy between Munc18b and Munc18a (Han et al., 2009). Third, when Munc18a levels are abundant in normal β -cells, this redundant action of Munc18b would not be or less asserted and thus less able to activate additional Syn-1A SNARE complexes to increase fusion of predocked SGs. This would also explain why predocked SG density on the PM in normal β -cells did not increase by the Munc18b overexpression.

3.5. Munc18b Restores the Deficient GSIS in GK Rat Islets to Normal Levels

The above human β -cell studies raise the potential that Munc18b could be deployed to treat T2D. We assessed this therapeutic potential of Munc18b in rescuing T2D *in vivo* by employing the GK rat model, wherein the abnormal glucose homeostasis is attributed almost entirely to a deficient GSIS from islets with little to no contribution from insulin resistance of peripheral tissues (Ostenson, 2001). We first examined the effects of the Munc18b rescue of GK rat islets *in vitro*. We previously reported that GK rat islets exhibit a similar reduction in levels of Munc18a, Syn-1A, VAMP2 and SNAP25 (Ostenson and Efendic, 2007; Gaisano et al., 2002) as in T2D human islets. Like human T2D islets (Fig. 1d), GK rat islets compared to Wistar rat islets (Fig. 5a) showed a similar reduction in Munc18b levels to 34% of normal levels. GK islet Syn-3 levels remained normal consistent with the T2D human islet result, whereas VAMP8 levels were reduced to 43% of normal compared normal VAMP8 levels in human T2D islets. GK rat β -cell is therefore an excellent model that mimics human T2D β -cell's exocytotic defects. *Ad*-Munc18b/eGFP (vs eGFP control) expression in GK rat islets raised Munc18b levels to five-fold of the original GK islet levels (Fig. 5b blots and bottom graph), when compared to Fig. 5a (GK rat islet Munc18b levels is 34% of normal Wistar rat islets). This led us to estimate that *Ad*-Munc18b infection raised GK rat islet levels to 170% ($5 \times 34\%$) of normal Wistar rat islet levels. This completely restored first- (first 15 min) and second-phase (15 min to 50 min) GSIS (Fig. 5c) to similar secretory responses of normal Wistar islets in first-phase (GK Munc18b: 6.02 ± 1.47 ; GK Control: 2.79 ± 0.39 ; Wistar: 4.14 ± 0.39) and second-phase GSIS (GK Munc18b: 12.17 ± 1.67 ; GK Control: 5.06 ± 0.23 ; Wistar: 11.94 ± 1.04). Munc18b overexpression did not affect the levels of any SNARE or other Munc18 proteins (Fig. 5b), suggesting that overexpressed Munc18b has to work with these more limiting amounts of SNARE proteins in GK islets.

We next examined what SG populations are deficient in GK rat β -cells and which could be rescued by Munc18b (Fig. 5d). In GK rat β -cells, the density of predocked SGs at resting condition was similar in trend as human T2D beta cells (GK Munc18b: 8.65 ± 0.88 , GK Control: 6.68 ± 0.87 , Wistar: 7.45 ± 1.04 , Fig. 5di), but their differences were not significant. Nonetheless, similar to human T2D β -cells (Fig. 4b), GK rat β -cells showed major reductions in fusions of predocked SGs (GK: 1.87 ± 0.61 ; Wistar: 3.86 ± 0.20 , Fig. 5dii, iii, v) and newcomer SGs in both first-phase (GK: 9.97 ± 1.85 , Wistar: 20.09 ± 4.16) and second-phase (GK: 8.08 ± 1.64 ; Wistar: 16.25 ± 4.71). Also like human T2D β -cells (Fig. 4b), in first-phase, Munc18b overexpression (Fig. 5b, 170% of normal Wistar rat islet levels) in GK rat β -cells fully recovered the deficient newcomer SGs (GK + Munc18b: 20.96 ± 4.14 ; GK: 9.97 ± 1.85 , Wistar: 20.09 ± 4.16) and remarkably, also greatly increased fusions of predocked SGs (GK + Munc18b: 5.96 ± 1.35 ; GK: 1.87 ± 0.61 ; Wistar: 3.86 ± 0.20). Moreover, Munc18b overexpression also fully recovered the deficient newcomer SGs (GK + Munc18b: 15.24 ± 2.85 ; GK: 8.08 ± 1.64 ; Wistar: 16.25 ± 4.71) in second-phase.

The explanations for the rescue of newcomer SGs by Munc18b overexpression in GK rat β -cells are as discussed for the T2D human β -cells. However, the increased fusion of predocked SGs in GK rat β -cells may not be attributed entirely to the (insignificant) reduction in the density of predocked SGs on the PM, but also contributed to the fusion defects *per se* of predocked SGs in T2D β -cells. Taking together the GK rat and human T2D β -cell results, it would seem that Munc18b overexpression-mediated rescue of T2D β -cell includes both an increase in the recruitment of additional predocked SGs to the PM and also a restoration of its fusion-readiness after they are docked onto the PM.

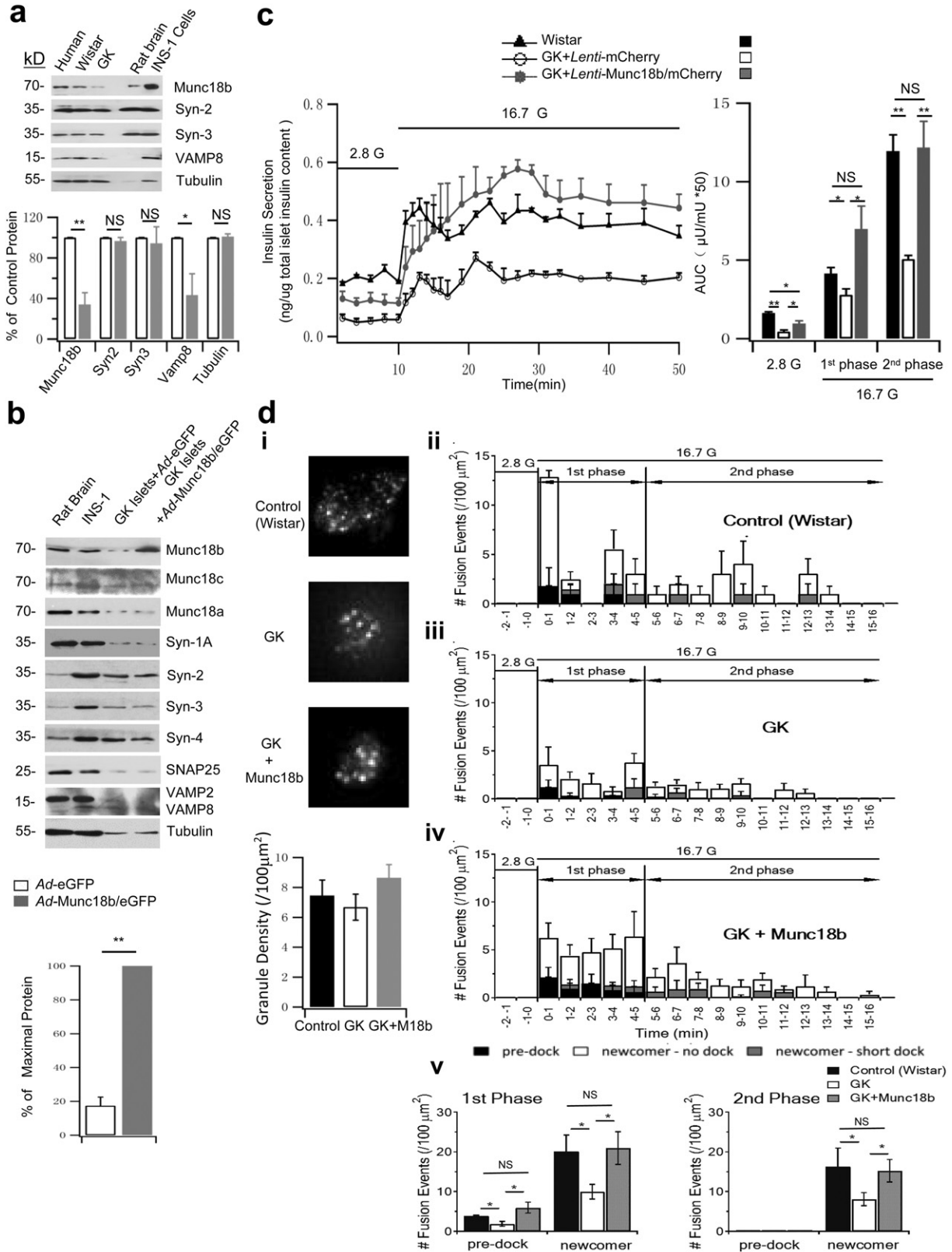
3.6. Munc18b-Enhanced GSIS Alleviates the Abnormal Glucose Homeostasis in GK Rats

The above studies showing Munc18b enhancement of GSIS suggests that Munc18b transduced *in vivo* into GK rat pancreatic islets would be expected to improve glucose homeostasis. We recently reported (Banks et al., 2014) that infusing a virus directly into the common biliopancreatic duct, with distal occlusion to the liver, could efficiently transduce the virus protein expression into pancreas, particularly islets. For validation, we confirm the efficiency of islet infection using this strategy by infusing *Ad*-Munc18b/eGFP into the pancreas of Wistar rats, then resected the pancreas 2 h after and isolated the islets, which were cultured for 1 and 2 days to monitor Munc18b/eGFP expression (Fig. S1a). Almost the entire islet (and almost all islets examined) was green at Day 2, including islet core where β -cells are concentrated. Maximal Munc18b/eGFP expression in the islets is shown by 3D reconstruction of these serial images at Day 2, with expected lower expression in Day 1. This indicates that most islets in the intact pancreas should be fully expressing Munc18b/eGFP by 1 week when we start to perform *in vivo* glucose homeostasis assays. For further validation, we performed survival operations on 3–4 month old Wistar rats (Fig. S1c) before proceeding to GK rats (Fig. 6) which underwent pancreatic ductal infusion with *Ad*-Munc18b/eGFP vs *Ad*-eGFP as control. We monitored both groups of rats by IPGTT up to 4 months post-op. In several Wistar rats, we isolated islets at 2 and 4 weeks post-op to monitor Munc18b/eGFP expression, which remained maximal at 2 weeks post-op (Fig. S1b).

Fig. 5. Munc18b restores the deficient GSIS in GK rat islets to normal levels. (a) Western blot analysis of Munc18b and cognate SNARE proteins in pancreatic islets of normal Wistar and GK rats. *Bottom:* Summary of densitometric analysis of blots from 3 separate experiments; results expressed as percentage of control values. (b) Western blot analysis of SM and SNARE proteins of *Ad*-Munc18b/eGFP and *Ad*-eGFP-transduced GK rat islets. Rat brain and INS-1 are positive controls. Data shown is representative of 3 sets of experiments. *Bottom:* densitometric analysis of Munc18b overexpression compared to *Ad*-eGFP-transduced GK rat islets ($N = 3$). Other proteins showed no change after Munc18b overexpression (analysis not shown). (c) Islet perfusion assays of *Lenti*-mCherry- and *Lenti*-Munc18b/mCherry-transduced GK rat islets, and *Lenti*-mCherry-transduced normal Wistar rat islets; and corresponding AUCs (right) of first-phase (10–25 min) and second-phase (25–50 min) insulin release. Data shown are from 3 sets of experiments. (d) TIRFM images showing SG density on the PM at basal condition (i, $N = 9$; scale bars represent 2 μm); *Bottom:* Comparison of averaged SG densities and histograms of the different fusion events after glucose-stimulation (ii–iv). First-phase (5 min after 16.7 mM glucose stimulation) and second-phase (5–16 min) in *Lenti*-mCherry-transduced Wistar rat β -cells (i, $N = 15$), and GK rat β -cells transduced with *Lenti*-mCherry (ii, $N = 17$) or *Lenti*-Munc18b/mCherry (iii, $N = 16$). Data obtained from 3 independent experiments. (v) Although (ii), (iii) and (iv) are shown in three modes of fusion (predocked, short-dock and no-dock newcomer SGs) events in first- and second-phase GSIS, the summary combined the two populations of newcomer SGs. Data are shown as mean \pm SEM, * $p < 0.05$; ** $p < 0.01$, NS: no significant difference.

top) similar to the *in vitro* islet culture at Day 2 (Fig. S1a). However, at 4 weeks post-op, Munc18b/eGFP expression remained strong albeit considerably less than at 2 weeks post-op; thus we expected further decline in Munc18b/eGFP expression after 4 weeks. In Ad-Munc18b/eGFP-infused Wistar rats (Fig. S1c), IPGTTs showed mildly lower glycemic responses at 1 week post-op (Munc18b/eGFP: 1129 ± 14.25 ; Control:

1498.06 ± 56.27), but this improved glycemic response was not sustained at 2 and 4 weeks post-op, likely because of adaptive responses of peripheral tissues to the increased insulin levels. Nonetheless, at 1 week post-op, we saw large increases in blood insulin levels encompassing first- and second-phase GSIS, where AUC analysis of bi-phasic GSIS showed a 48% increase (Munc18b/eGFP: 279.18 ± 19.47 ;



Control: 189.51 ± 2.16). This increase in GSIS *in vivo* was less pronounced at 2 and 4 weeks post-op and observed only at latter time points (*i.e.* 30 min) consistent with the reduced Munc18b/eGFP expres-

sion at 4 weeks (Fig. S1b *bottom*).

GK rats (Stockholm colony) at 3–4 months predictably developed hyperglycemia (Ostenson, 2001) (Fig. 6a, GK: 3183.35 ± 177.36 ;

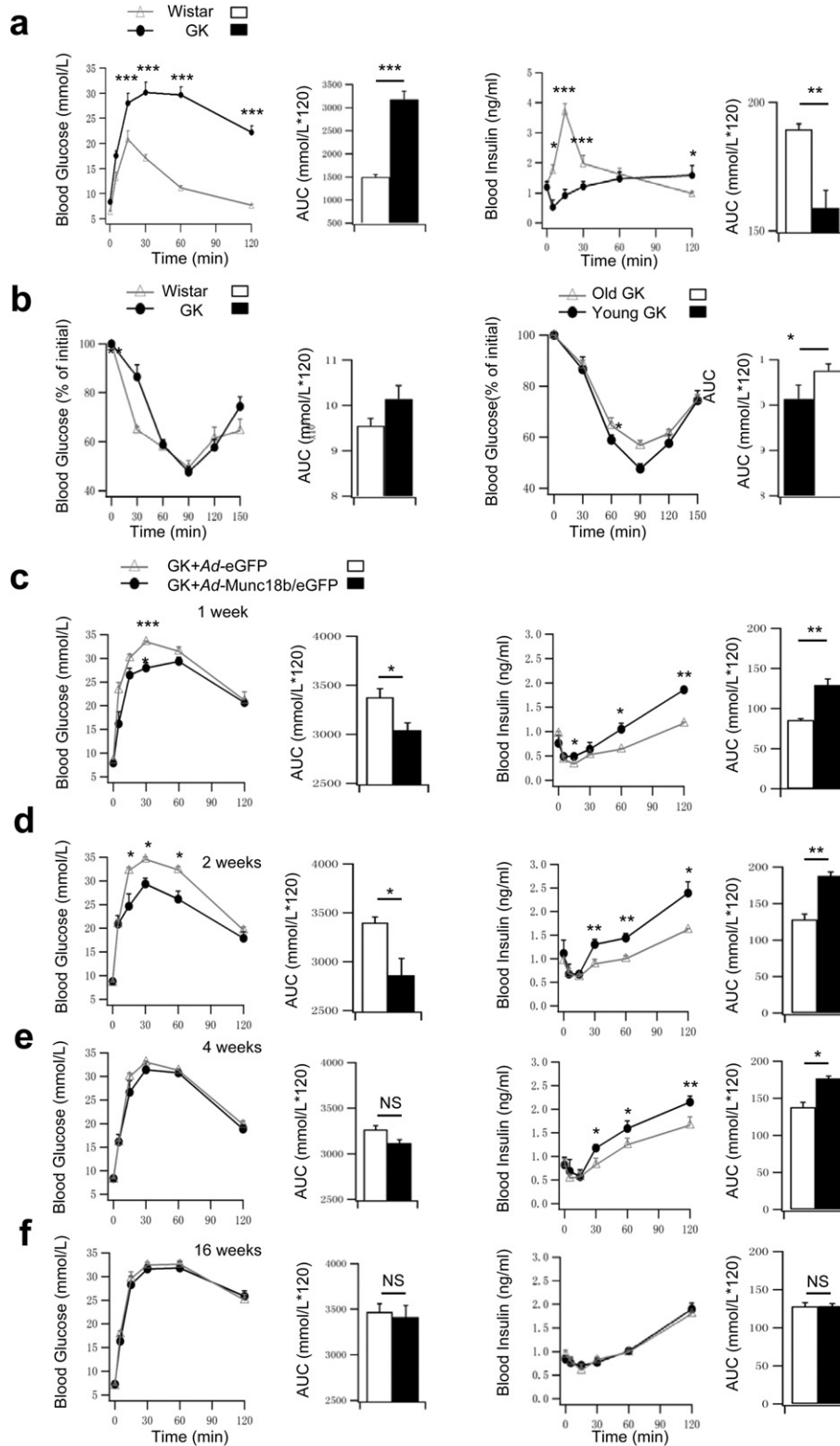


Fig. 6. Infusion of Ad-Munc18b into the pancreas of T2D GK rats improves glucose homeostasis. (a) IPGTTs performed on age-matched Wistar and GK rats. Blood glucose (left) and insulin levels (right) are shown along with the AUCs encompassing 120 min of the IPGTT. N = 5 for each group. (b) IPITTs performed. Left: age-matched Wistar (N = 7) vs GK rats (N = 5). Right: Young (14 week old, N = 5) vs old (20 week old, N = 4) GK rats. Blood glucose results shown as percentage of initial levels along with AUCs encompassing 150 min of the IPITT. (c–f) Ad-Munc18b/eGFP vs Ad-eGFP infused via pancreatic duct into GK rats. IPGTTs (blood glucose (left), insulin levels (right)) performed post-op at 1 week (c), 2 weeks (d), 4 weeks (e) and 16 weeks (f). AUCs encompassing 120 min of the IPGTTs are shown. Ad-eGFP: N = 5 for 1 and 2 weeks, N = 4 for 4 and 16 weeks. Ad-Munc18b/eGFP: N = 6 for 1 and 2 weeks, N = 5 for 4 weeks, and N = 4 for 16 weeks. Data are shown as mean \pm SEM; *p < 0.05, **p < 0.01, ***p < 0.001, NS: no significant difference.

Wistar: 1498.06 ± 56.27) with greatly reduced insulin release (AUC analysis of biphasic GSIS, GK: 159 ± 25.67 ; Wistar: 190 ± 2.16), particularly at early time points of first-phase GSIS (0–30 min) typical of T2D. Insulin tolerance tests showed similar results between GK and Wistar rats (Fig. 6b), confirming that hyperglycemia in GK rats was attributed mainly to β -cell insulin secretory deficiency with little contribution from peripheral tissue insulin resistance (Ostenson, 2001). After Ad-Munc18b/eGFP pancreatic infusion, IPGTTs performed on these GK rats showed greatly improved glycemic responses at 1 and 2 weeks post-op along with large increases in blood insulin levels, particularly at the latter time points (30–120 min in Fig. 6c, d) encompassing second-phase GSIS. While the enhanced insulin secretion in Ad-Munc18b/eGFP-treated GK rats was still observed, albeit less at 4 weeks postop (Fig. 6e), the glycemic responses were similar to Control (Ad-eGFP-treated) GK rats. At 16 weeks post-op (Fig. 6f), glycemic and insulin responses were similar between the two groups since much of the Ad-Munc18b/eGFP expression would not have persisted that long (Fig. S1b bottom). Lastly, Ad-Munc18b/eGFP overexpression (compared to Ad-eGFP) did not affect islet β -cell mass or total pancreatic insulin content in GK rats at 2 weeks and 17 weeks post-op (Fig. S2), indicating that changes in *in vivo* insulin secretory capacity were attributed to Munc18b actions on single β -cell secretory output.

4. Discussion

Although much is known about β -cell SNARE proteins and how they contribute to islet secretory deficiency in T2D, this is the first work to demonstrate that these insights could be translated into potential therapies for T2D. Of the many SM/SNARE proteins that showed reduced levels in T2D islets, we chose to rescue the reduced levels of Munc18b. A major reason is that non-stoichiometric increases in a SNARE protein (*i.e.* Syn-1A) would actually reduce insulin secretion (Lam et al., 2005) perhaps by inducing excess formation of incomplete non-fusogenic SNARE complexes. In contrast, slight excess in overexpression of a SM protein (~2.6X of normal levels in this study) would activate native levels of cognate SNARE proteins to form additional fusion-competent SM/SNARE complexes. We proposed Munc18b to be a preferred target since levels of its cognate SNARE proteins are either mildly (VAMP8) or not reduced (Syn-3) in T2D islets, whereas levels of SNARE proteins preferentially activated by Munc18a are generally more reduced (Syn-1A, VAMP2, SNAP25). Consistently, we had reported that Munc18b depletion in rat islets disabled Syn-3/VAMP8/SNAP25 SNARE complex assembly resulting in reduced biphasic GSIS (Lam et al., 2013). The additional Munc18b/SNARE complexes induced to form by Munc18b overexpression would be sensitive to current therapies acting on cAMP (*i.e.* glucagon-like peptide-1 drugs) (Lam et al., 2013) and calcium (Mandic et al., 2011) (*i.e.* sulfonylureas) signaling pathways. We had reported that Munc18b and Munc18a exhibited functional redundancy in their actions on Syn-1A, -2 and -3 (Han et al., 2009) and this will likely be able activate each other's preferred SNARE complexes. This suggests the interesting possibility that Munc18a overexpression might likewise mount a similar rescue as Munc18b.

By showing that pancreatic ductal perfusion of Ad-Munc18b attained a sustained improvement of glucose homeostasis in T2D GK rats, our study raises the possibility of employing this strategy in human subjects by endoscopy as a potential treatment for T2D patients. Adenovirus, whose effects lasted <4 months, is of course not the ideal gene transfer strategy; and a longer-acting and safer gene transfer approach as was recently shown with adeno-associated virus (subtype 8) (Gaddy et al., 2012) will be required for humans trials. *Ex vivo* transduction of Munc18b expression into normal islets could be deployed in islet transplantation protocols, whereby surviving islets post-transplantation would be more efficient secretors, thus metabolic demand would be less exhausting on the limited β -cell mass. Of note, the overall glycemic improvement in our GK rat study did not reach normoglycemia likely because of some reduction in β -cell mass, or more likely the Ad-

Munc18b transduction did not reach all the islets in the pancreas. Our initial attempts to infuse more Ad-Munc18b into the rat pancreatic ducts resulted in pancreatitis and higher mortality. This thinking is in part supported by lower islet perfusion responses in human T2D islets wherein the Ad-Munc18b expression in the larger human T2D human islets did not reach the islet cores.

Munc18b is also found in epithelial cells including mucin-secreting airway cells (Kim et al., 2012) and blood cells including mast cells (Kim et al., 2012) and platelets (Al Hawas et al., 2012). Munc18b deficiency in these cells resulted in secretory defects that can cause corresponding lung, allergy and bleeding disorders. More work is required to assess the structure-function of Munc18b and how such could modulate the ability of Munc18b to form distinct SNARE complexes (Al Hawas et al., 2012; Kauppi et al., 2002; Han et al., 2009) that could assert cell context-selective effects on secretion, whether to therapeutically promote secretion (β -cells in T2D, lung mucin production in cystic fibrosis), inhibit secretion (mast cells in anaphylaxis), or both (platelet-acting drugs). Specifically, in β -cells (and neurons), Takahashi et al. (2015) recently showed by two-photon lifetime imaging that the trans-SNARE complex (Syn-1A, SNAP25, VAMP2) is not formed at resting state, but becomes assembled only shortly prior to insulin exocytosis. This approach could be used to assess the states of assembly of Munc18b with and among its cognate SNARE proteins (Syn-3, VAMP8), and how different they may be from Munc18a/SNARE complex assembly in explaining the distinct states of fusion readiness between predocked and newcomer SGs.

Supplementary data to this article can be found online at <http://dx.doi.org/10.1016/j.ebiom.2017.01.030>.

Conflict of Interest Statement

The authors declare no actual or potential competing financial interests.

Author Contributions

T.Q., T.L. and D.Z. designed and performed most of the experiments and data analysis. K.B. developed and supervised the surgical technique. Y.K., L.X. and S.D. contributed to some experiments and data analysis. S.S. and N.T. provided most of the virus constructs; C.-G.O. provided the original GK colony. T.Q. and H.Y.G. wrote the manuscript. All authors edited and approved the final version of the manuscript.

Acknowledgements and Funding Sources

This research was supported by a grant from the Canadian Institutes of Health Research (CIHR) MOP-119352 and postdoctoral fellowships provided support to D.Z. (Banting and Best Diabetes Centre, University of Toronto), L.X. (Canadian Diabetes Association) and S.D. (Canadian Association of Gastroenterology and CIHR). There is no conflict of interests.

References

- Al Hawas, R., Ren, Q., Ye, S., Karim, Z.A., Filipovich, A.H., Whiteheart, S.W., 2012. Munc18b/STXBP2 is required for platelet secretion. *Blood* 120, 2493–2500.
- Banks, K., Qin, T., Liang, T., Wang, A.J., Gaisano, H.Y., 2014. Biliopancreatic route for effective viral transduction of pancreatic islets. *Pancreas* 43, 240–244.
- Gaddy, D.F., Riedel, M.J., Bertera, S., Kieffer, T.J., Robbins, P.D., 2012. dsAAV8-mediated gene transfer and β -cell expression of IL-4 and β -cell growth factors are capable of reversing early-onset diabetes in NOD mice. *Gene Ther.* 19, 791–799.
- Kwan, E.P., Gaisano, H.Y., 2009. Rescuing the subprime meltdown in insulin exocytosis in diabetes. *Ann. N.Y. Acad. Sci.* 1152, 154–164.
- Gaisano, H.Y., 2014. Here come the newcomers granules, better late than never. *Trends Endocrinol. Metab.* 25, 381–388.
- Gaisano, H.Y., Ostenson, C.G., Sheu, L., Wheeler, M.B., Efendic, S., 2002. Abnormal expression of pancreatic islet exocytotic soluble N-ethylmaleimide-sensitive factor attachment protein receptors in Goto-Kakizaki rats is partially restored by phlorizin treatment and accentuated by high glucose treatment. *Endocrinology* 143, 4218–4226.
- Han, L., Jiang, T., Han, G.A., Malintan, N.T., Xie, L., Wang, L., Tse, F.W., Gaisano, H.Y., Collins, B.M., Meunier, F.A., et al., 2009. Rescue of Munc18-1 and -2 double knock-down

- reveals the essential functions of interaction between Munc18 and closed syntaxin in PC12 cells. *Mol. Biol. Cell* 20, 4962–4975.
- Hosker, J.P., Rudenski, A.S., Burnett, M.A., Matthews, D.R., Turner, R.C., 1989. Similar reduction of first- and second-phase B-cell responses at three different glucose levels in type II diabetes and the effect of gliclazide therapy. *Metabolism* 38, 767–772.
- Jewell, J.L., Oh, E., Thurmond, D.C., 2010. Exocytosis mechanisms underlying insulin release and glucose uptake: conserved roles for Munc18c and syntaxin 4. *Am. J. Physiol. Regul. Integr. Comp. Physiol.* 298, R517–R531.
- Kasai, H., Takahashi, N., Tokumaru, H., 2012. Distinct initial SNARE configurations underlying the diversity of exocytosis. *Physiol. Rev.* 92, 1915–1964.
- Kauppi, M., Wohlfahrt, G., Olkkonen, V.M., 2002. Analysis of the Munc18b-syntaxin binding interface. Use of a mutant Munc18b to dissect the functions of syntaxins 2 and 3. *J. Biol. Chem.* 277, 43973–43979.
- Kim, K., Petrova, Y.M., Scott, B.L., Nigam, R., Agrawal, A., Evans, C.M., Azzegagh, Z., Gomez, A., Rodarte, E.M., Olkkonen, V.M., et al., 2012. Munc18b is an essential gene in mice whose expression is limiting for secretion by airway epithelial and mast cells. *Biochem. J.* 446, 383–394.
- Kwan, E.P., Gaisano, H.Y., 2005. Glucagon-like peptide 1 regulates sequential and compound exocytosis in pancreatic islet β -cells. *Diabetes* 54, 2734–2743.
- Lam, P.P., Leung, Y.M., Sheu, L., Ellis, J., Tsushima, R.G., Osborne, L.R., Gaisano, H.Y., 2005. Transgenic mouse overexpressing syntaxin-1A as a diabetes model. *Diabetes* 54, 2744–2754.
- Lam, P.P., Ohno, M., Dolai, S., He, Y., Qin, T., Liang, T., Kang, Y., Liu, Y., Kauppi, M., Xie, L., et al., 2013. Munc18b is a major mediator of insulin exocytosis in rat pancreatic β -cells. *Diabetes* 62, 2416–2428.
- Mandic, S.A., Skelin, M., Johansson, J.U., Rupnik, M.S., Berggren, P.O., Bark, C., 2011. Munc18-1 and Munc18-2 proteins modulate β -cell Ca²⁺ sensitivity and kinetics of insulin exocytosis differently. *J. Biol. Chem.* 286, 28026–28040.
- Oh, E., Kalwat, M.A., Kim, M.J., Verhage, M., Thurmond, D.C., 2012. Munc18-1 regulates first-phase insulin release by promoting granule docking to multiple syntaxin isoforms. *J. Biol. Chem.* 287, 25821–25833.
- Ohara-Imaizumi, M., Nishiwaki, C., Kikuta, T., Nagai, S., Nakamichi, Y., Nagamatsu, S., 2004. TIRF imaging of docking and fusion of single insulin granule motion in primary rat pancreatic beta-cells: different behavior of granule motion between normal and Goto-Kakizaki diabetic rat beta-cells. *Biochem. J.* 381, 13–18.
- Ohara-Imaizumi, M., Fujiwara, T., Nakamichi, Y., Okamura, T., Akimoto, Y., Kawai, J., Matsushima, S., Kawakami, H., Watanabe, T., Akagawa, K., et al., 2007. Imaging analysis reveals mechanistic differences between first- and second-phase insulin exocytosis. *J. Cell Biol.* 177, 695–705.
- Orci, L., Malaisse, W., 1980. Hypothesis: single and chain release of insulin secretory granules is related to anionic transport at exocytotic sites. *Diabetes* 29, 943–944.
- Ostenson, C.G., 2001. The Goto-Kakizaki rat. In: Sima, A.A.F., Shafir, E. (Eds.), *Animal Models in Diabetes: A Primer*. Harwood Academic Publishers, Amsterdam, pp. 197–211.
- Ostenson, C.G., Efendic, S., 2007. Islet gene expression and function in type 2 diabetes: studies in the Goto-Kakizaki rat and humans. *Diabetes Obes. Metab.* 9, 180–186.
- Ostenson, C.G., Gaisano, H.Y., Sheu, L., Tibell, A., Bartfai, T., 2006. Impaired gene and protein expression of exocytotic soluble N-ethylmaleimide attachment protein receptor complex proteins in pancreatic islets of type 2 diabetic patients. *Diabetes* 55, 435–440.
- Ostenson, C.G., Chen, J., Sheu, L., Gaisano, H.Y., 2007. Effects of palmitate on insulin secretion and exocytotic proteins in islets of diabetic Goto-Kakizaki rats. *Pancreas* 34, 359–363.
- Riento, K., Jantti, J., Jansson, S., Hielm, S., Lehtonen, E., Ehnholm, C., Keranen, S., Olkkonen, V.M., 1996. A sec1-related vesicle-transport protein that is expressed predominantly in epithelial cells. *Eur. J. Biochem.* 239, 638–646.
- Rorsman, P., Renstrom, E., 2003. Insulin granule dynamics in pancreatic β -cells. *Diabetologia* 46, 1029–1045.
- Shibasaki, T., Takahashi, H., Miki, T., Sunaga, Y., Matsumura, K., Yamanaka, M., Zhang, C., Tamamoto, A., Satoh, T., Miyazaki, J., et al., 2007. Essential role of Epac2/Rap1 signaling in regulation of insulin granule dynamics by cAMP. *Proc. Natl. Acad. Sci. U. S. A.* 104, 19333–19338.
- Sudhof, T.C., Rothman, J.E., 2009. Membrane fusion: grappling with SNARE and SM proteins. *Science* 323, 474–477.
- Takahashi, N., Hatakeyama, H., Okado, H., Miwa, A., Kishimoto, T., Kojima, T., Abe, T., Kasai, H., 2004. Sequential exocytosis of insulin granules is associated with redistribution of SNAP25. *J. Cell Biol.* 165, 255–262.
- Takahashi, N., Hatakeyama, H., Okado, H., Noguchi, J., Ohno, M., Kasai, H., 2010. SNARE conformational changes that prepare vesicles for exocytosis. *Cell Metab.* 12, 19–29.
- Takahashi, N., Sawada, W., Noguchi, J., Watanabe, S., Ucar, H., Hayashi-Takagi, A., Yagishita, S., Ohno, M., Tokumaru, H., Kasai, H., 2015. Two-photon fluorescence lifetime imaging of primed SNARE complexes in presynaptic terminals and β -cells. *Nat. Commun.* 6, 8531.
- Xie, L., Zhu, D., Dolai, S., Liang, T., Qin, T., Kang, Y., Huang, Y.C., Gaisano, H.Y., 2015. Syntaxin-4 mediates exocytosis of pre-docked and newcomer insulin granules underlying biphasic glucose stimulated insulin secretion in human pancreatic beta cells. *Diabetologia* 58, 1250–1259.
- Zhu, D., Zhang, Y., Lam, P.P., Dolai, S., Liu, Y., Cai, E.P., Choi, D., Schroer, S.A., Kang, Y., Allister, E.M., et al., 2012. Dual role of VAMP8 in regulating insulin exocytosis and islet β -cell growth. *Cell Metab.* 16, 238–239.
- Zhu, D., Koo, E., Kwan, E., Kang, Y., Park, S., Xie, H., Sugita, S., Gaisano, H.Y., 2013. Syntaxin-3 regulates newcomer insulin granule exocytosis and compound fusion in pancreatic β -cells. *Diabetologia* 56, 359–369.
- Zhu, D., Xie, L., Karimian, N., Liang, T., Kang, Y., Huang, Y.C., Gaisano, H.Y., 2015. Munc18c mediates exocytosis of pre-docked and newcomer insulin granules underlying biphasic glucose stimulated insulin secretion in human pancreatic beta-cells. *Mol. Metab.* 4, 418–426.